Int. J. Electrochem. Sci., 13 **(2018)** 10809 – 10820, doi: 10.20964/2018.11.59

International Journal of ELECTROCHEMICAL SCIENCE
www.electrochemsci.org

Novel Ginger-like Morphology of Barium Molybdate: A Promising Electrocatalyst for the Detection of Neurotransmitter Dopamine

Periyasamy Sundaresan[1], *Yu Chi Chen*[1], *Shen-Ming Chen*[1,*], *Tse-Wei Chen*[1,2], *Petchi Latha*[3], *and Bih-Show Lou*[4,5*],

[1] Electroanalysis and Bioelectrochemistry Lab, Department of Chemical Engineering and Biotechnology, National Taipei University of Technology, No.1, Section 3, Chung-Hsiao East Road, Taipei 106, Taiwan, ROC.
[2] Research and Development Center for Smart Textile Technology, National Taipei University of Technology, No. 1, Section 3, Chung-Hsiao East Road, Taipei 106, Taiwan, ROC.
[3] Department of Chemistry, VHNSN College, Virudhunagar-626001, Tamil Nadu, India.
[4] Chemistry Division, Center for General Education, Chang Gung University, Taoyuan, Taiwan,
[5] Department of Nuclear Medicine and Molecular Imaging Center, Chang Gung Memorial Hospital, Taoyuan, Taiwan
[*]E-mail: smchen78@ms15.hinet.net, blou@mail.cgu.edu.tw

Received: 20 July 2018 / *Accepted:* 22 August 2018 / *Published:* 1 October 2018

In this work, we have report a novel electrochemical sensor for the selective detection of dopamine (DA) based on ginger-like morphology of barium molybdate ($BaMoO_4$; BaM) modified screen printed carbon electrode (SPCE). The ginger-like BaM was prepared through a simple co-precipitation technique and its physiochemical properties were systematically investigated by various analytical and spectroscopic techniques such as X-ray diffraction (XRD), Raman, field emission-scanning electron microscopy (FE-SEM) and energy-dispersive X-ray spectroscopy (EDX). Furthermore, the as-prepared ginger-like BaM was effectively investigated for the sensitive and selective electrochemical determination of DA. The ginger-like BaM/SPCE shows a reversible electrochemical behavior with superior current response for DA detection. The BaM catalyst played a significant role to electrochemical detection of DA, as a results very low detection limit (0.021 μM), wide linear response range (0.1-266 μM), well sensitivity (0.35 $\mu A \mu M^{-1} cm^{-2}$) and good selectivity in the presence of common metal ions and biological compounds. This study provides a novel idea for the fabrication of binary metal oxides and their potential application in electrochemical sensor and biosensor.

Keywords: Binary metal oxide, Ginger-like, Barium molybdate, Neurotransmitter, Dopamine, Electrochemical sensor

1. INTRODUCTION

Recent years, transition metal molybdate poses great attention in numerous areas including photocatalysis, electrocatalysis, supercapacitors, lithium-ion batteries, and luminescent material, etc., owing to their superior physicochemical properties [1-7]. In particular, scheelite-type molybdates ($AMoO_4$; A= Ni, Co, Pb, Sr, Ba, etc.,) has received tremendous interest in catalysis, photocatalysis, optoelectronic devices, scintillators, anode material and so forth [8-11]. Among the scheelite-type molybdates, barium molybdate ($BaMoO_4$; BaM), is one of the significant in catalyst, scintillators of medical devices, fiber-optics, electrocatalyst, solar cells, solid-state lasers, light emitting diodes. Therefore, various researchers have paid immense attention for the synthesis of $BaMoO_4$ through different techniques such as solid-state synthesis, electrochemical deposition, solution combustion method, microemulsion technique, co-polymerization, solvothermal route, molten-salt synthesis and microwave-assisted techniques [12-19]. However, there are no reports available for the synthesis of ginger-like BaM via a simple (i.e., Co-precipitation) technique and its application for the electrochemical detection of dopamine.

Dopamine (DA) is one of the families of catecholamine which normally occurs in central nervous system. Further, the DA acts as an essential role in human body such as mental and emotional activity, metabolism and neurotransmission. However, low or high concentration level of DA in human body can causes severe health risks including HIV infection, dementia and senile diseases. For these reasons, the accurate determination of DA level in human body is necessary concern to the researchers. Up to now, a number of analytical techniques such as fluorescence, calorimetry, surface enhanced Raman spectroscopy (SERS), chemiluminescence and chromatography have been successfully developed for the accurate and low level detection of DA [20-28]. However, the aforesaid methods have some disadvantages such as high cost instrument, usage in expensive solvents, needed huge amount of reagents, hard to operate, and time consuming process. Conversely, electrochemical technique could provide low cost, easy to handling, high sensitivity, good selectivity and easily portable when compared to aforementioned traditional methods [29].

Herein, we have developed a novel electrochemical sensor for the detection of DA based on ginger-like BaM modified SPCE for the first time. The as-prepared BaM was effectively confirmed by different analytical and spectroscopic techniques. The as-prepared BaM/SPCE was employed as an electrocatalyst for the detection of DA. Compared to the unmodified electrode, the electrochemical behavior of DA in BaM/SPCE has effectively improved. Several influential factors such as effect of scan rate and pH were investigated.

2. EXPERIMENTAL SECTION

2.1 Materials

Barium sulfate ($BaSO_4$), sodium molybdate dihydrate ($Na_2MoO_4.2H_2O$), dopamine (DA), hydrazine (HYD), hydrogen peroxide (H_2O_2), hydroquinone (HQ), caffeic acid (CA), catechol (CC), sodium chloride (NaCl), potassium chloride (KCl), uric acid (UA), ascorbic acid (AA), glucose

(GLU), and monosodium dihydrogen phosphate (NaH_2PO_4), disodium hydrogen phosphate (Na_2HPO_4) for the preparation of phosphate buffer solution (0.05 M PBS) and all other chemicals were received from Sigma-Aldrich chemical Co., (USA), Alfa-Aeser (USA) and Fluka chemicals (Switzerland) companies. All the chemicals and solvents were of analytical grade and used without further purification. All required solutions were prepared by double distilled (DD) water.

2.2 Characterizations

The powder X-ray diffraction (XRD) analysis was recorded using XPERT-PRO spectrometer (PANalytical B.V., The Netherlands) with Cu-Ka radiation λ = 1.5406 Å. The Raman spectrum was acquired using a Raman spectrometer (Dong Woo 500i, Korea) equipped with a charge-coupled detector. The morphological studies of BaM were carried out with field emission-scanning electron microscopy (FE-SEM, Quanta 250, FEG, Hitachi, Japan operated at 15 kV). All the electrochemical studies of DA determination such as cyclic voltammetry (CV) and differential pulse voltammetry (DPV) were performed using CHI 1205 and CHI 900 (CH Instruments, USA) electrochemical workstation. A conventional three-electrode system was used for the electrochemical studies, where the modified ginger-like BaM screen printed carbon electrode (SPCE) was used as a working electrode (working area = 0.079 cm^2) and Ag/AgCl (sat. KCl) and platinum wire are used as reference and counter electrode, respectively. All the electrochemical measurements were carried out at room temperature with N_2 atmospheric conditions.

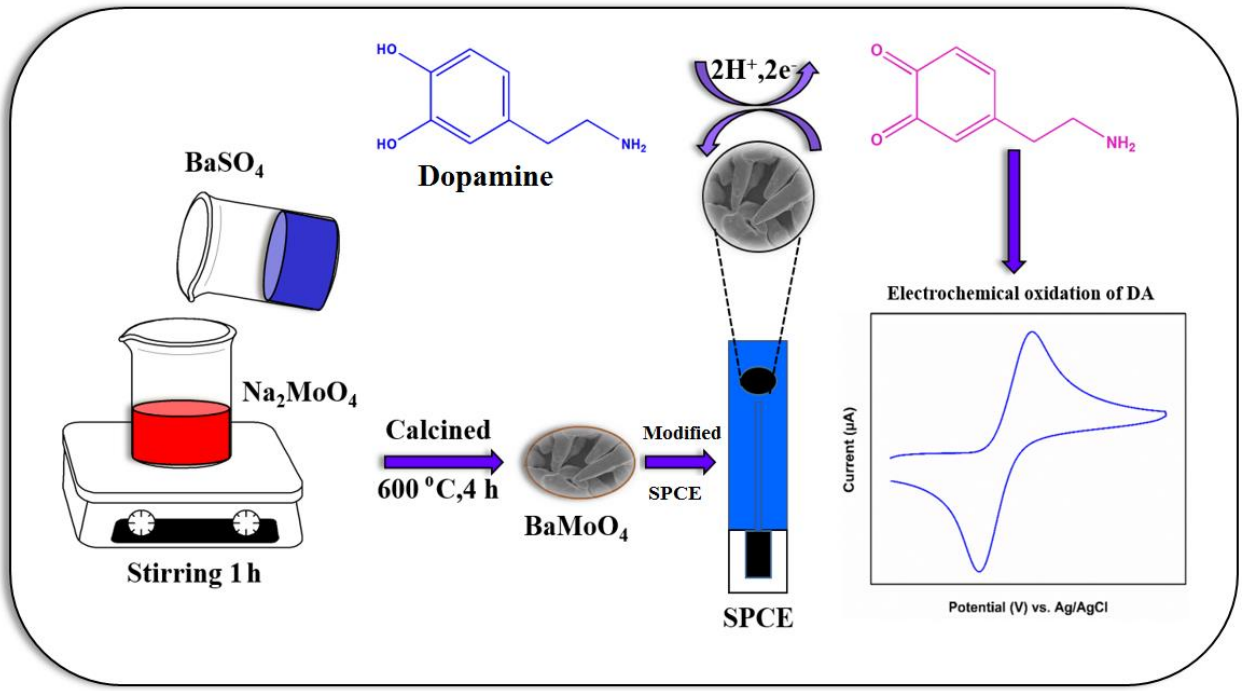

Scheme 1. The synthesis and fabrication of ginger-like BaM on the SPCE and its electrochemical applications towards DA detection.

2.3 Preparations of ginger-like $BaMoO_4$

The ginger-like $BaMoO_4$ were synthesized by a simple co-precipitation method [30]. In a typical procedure, 40 mL of 0.2 M (1.935 g) of Na_2MoO_4 was dissolved in a 250 mL beaker and allowed to stirring at room temperature, then, 40 mL of 0.1 M (0.832 g) of $BaSO_4$ solution was added into the above solution with continuously stirring for an hour. After that, the white precipitate ($BaMoO_4$) was washed with copious amount of DD water followed by ethanol and dried at 40 ^oC for overnight; finally, ginger-like $BaMoO_4$ was annealed at 600 ^oC for 4 h. Later, the annealed ginger-like $BaMoO_4$ was used for further physicochemical characterization and stored in a screw cap bottle when not in use.

2.4 Fabrication of ginger like $BaMoO_4$ modified SPCE

Prior to electrode modification process, the unused SPCE was washed with DD water and ethanol to remove the adsorbed impurities on the electrode surface. After that, 5 mg of as-prepared ginger like BaM was weighted and transferred into 1 mL of DD and ultrasonication for 15 min to get a homogeneous suspension. Then, 6 µL (optimized concentration) of ginger-like BaM homogeneous suspension was drop casted on the cleaned SPCE surface. After that, BaM drop casted SPCE was dried at ambient temperature in oven. Later, the dried electrode was gently washed with DD water to remove the loosely attached molecules on the SPCE surface. The obtained electrode was denoted as BaM/SPCE and it was used for all the electrochemical studies. The synthesis and fabrication of ginger like BaM on the SPCE and its electrochemical applications are shown in Scheme 1.

3. RESULTS AND DISCUSSION

3.1 Characterization of ginger-like BaM

The crystal structure of the as-prepared material was identified by XRD analysis and shown in Fig.1A. The observed diffraction peaks at 2θ= 29.63, 32.9, 35.13, 48.88, 50.3, 56.62, 38.47, and 59.5 were attributed to (112), (004), (200), (204), (220), (116), (312) and (224) miller indices planes of tetragonal phase of $BaMoO_4$ and is good consistent with the JCPDS No. 08−0455 [30-32]. No other notable peaks corresponds to the impurities were observed, suggested that the high purity of $BaMoO_4$. Raman spectrum of the as-prepared ginger-like BaM displayed in Fig.1B, the high intense peaks at 823, 761 and 717 cm^{-1}, ascribed to the Mo=O stretching, Mo-O-Mo symmetric and asymmetric stretching vibrations of $BaMoO_4$, respectively. The peaks at 231 and 266 cm^{-1} were corresponding to the Mo=O bending and distorted deformation Mo-O-Mo vibrations [33-35]. The FE-SEM micrographs in Fig.1C clearly demonstrate the ginger-like structure of as-prepared $BaMoO_4$. The average diameter and length of ginger-like BaM is to be 60 and 400 µm, respectively. The EDX spectrum of BaM (Fig.1D) exhibits that the only existing elements are Ba, Mo and O. No peaks of any impurity are observed in Fig.1D, indicating the high purity of the product.

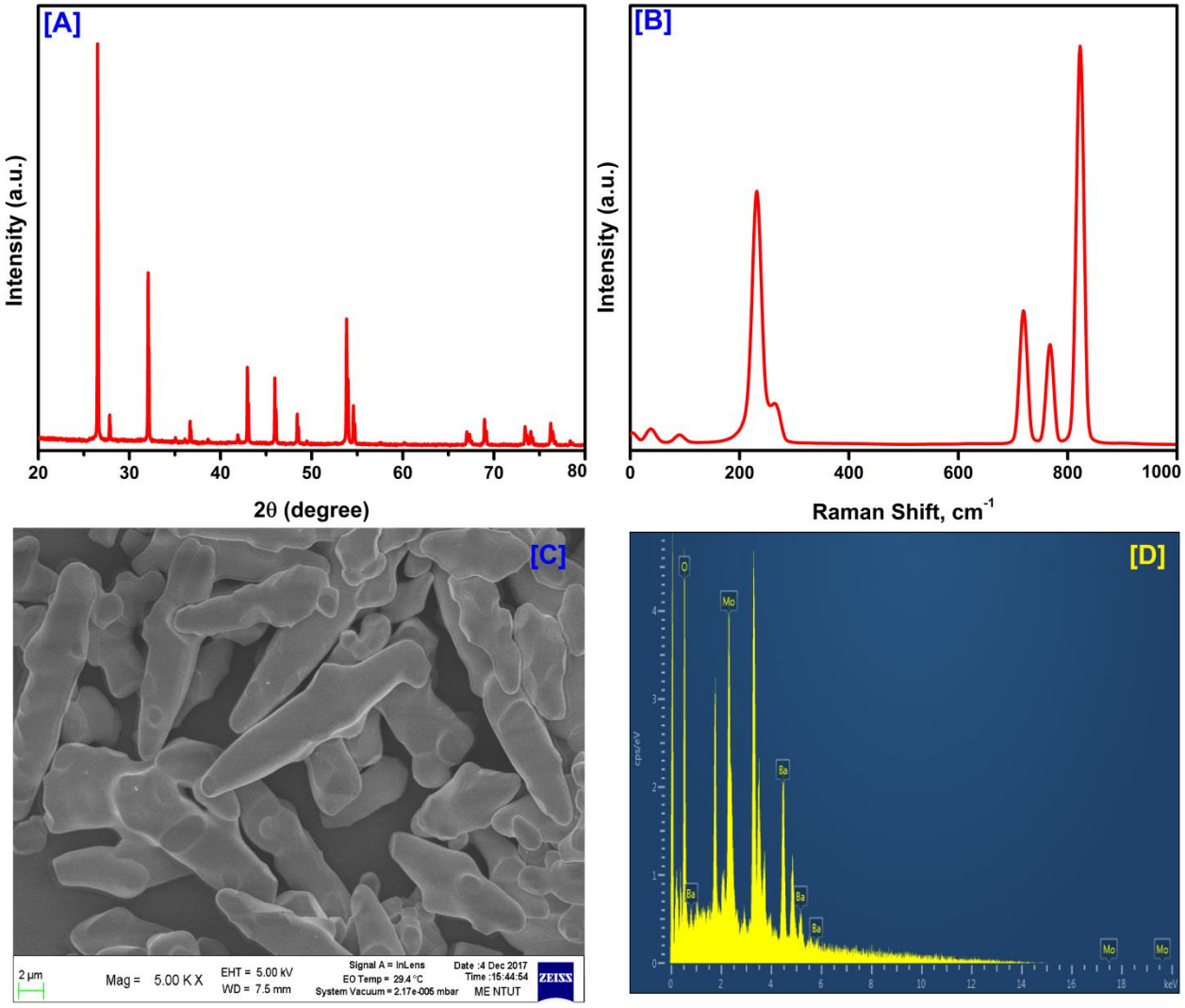

Figure 1. XRD (A), Raman (B), FE-SEM images of as-prepared BaM (C) and their corresponding EDX spectrum (D).

3.2 Electrochemical activity of BaM modified SPCE and unmodified SPCE

The electrochemical sensing properties of ginger-like BaM/SPCE and bare SPCE were investigated by CV for the detection of neurotransmitter DA (200 µM) in phosphate buffer solution (0.05 M PBS; pH 7.0) at a scan rate of 50 mV/s. Fig.2A shows the CV responses of ginger-like BaM/SPCE and bare SPCE in the presence (b, a) and absence (c, d) of 200 µM DA in 0.05 M PBS (pH 7). The bare SPCE and ginger-like BaM modified SPCE reveals that there is no electrochemical current signal was observed in the absence of 200 µM DA at the selected potential window ranging from -0.1 to + 0.7 V. However, an obvious and well-defined reversible redox peaks were observed on the BaM/SPCE at a scan rate of 50 mV/s with the current value of 6.15 µA, when the 200 µM of DA was added into 0.05 M PBS (pH 7.0). At the same time, the unmodified SPCE exhibits poor electrocatalytic activity comparatively lower to the BaM/SPCE. However, the obtained anodic peak is ascribed to the oxidation of DA to o-dopaminoquinone (DOQ), whereas, the cathodic peak is due to the reduction of DOQ to DA. The possible electrochemical redox mechanism of DA on the BaM/SPCE is shown in Scheme 2.

The obtained electrochemical results are clearly suggested that the ginger-like BaM has a higher active surface area and these larger surface areas is very helpful to improve the electrocatalytic activity of DA detection.

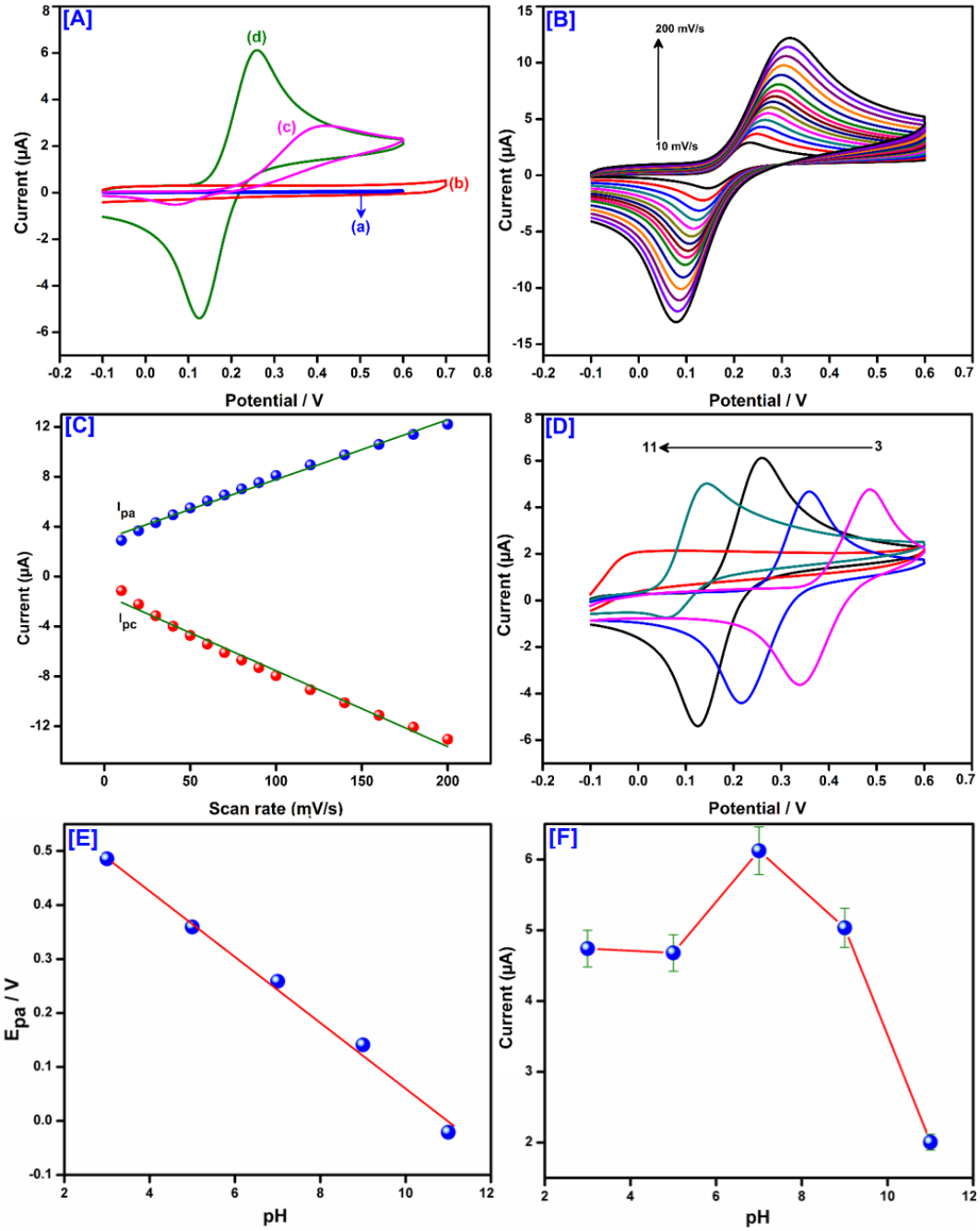

Figure 2. CV response of bare SPCE (a) and BaM modified SPCE (b) in the absence (a, b) and the presence of (c, d) of 200 μM DA in 0.05 M PBS (pH 7.0) at a scan rate of 50 mV/s (A). CV curves at BaM/SPCE with various scan rate ranging from 20 to 200 mV/s containing 0.05 PBS (pH 7.0; 200 μM DA) (B). The linear plot for the peak current (I_{pa} and I_{pc}) *vs.* scan rate (C). CV response for 200 μM DA at BaM/SPCE with various pH values from 3.0 to 11.0 at a scan rate of 50 mV/s (D). The linear relationship between the peak potential *vs.* pH (E) and The calibration plot for the anodic peak current *vs.* different pH value (F).

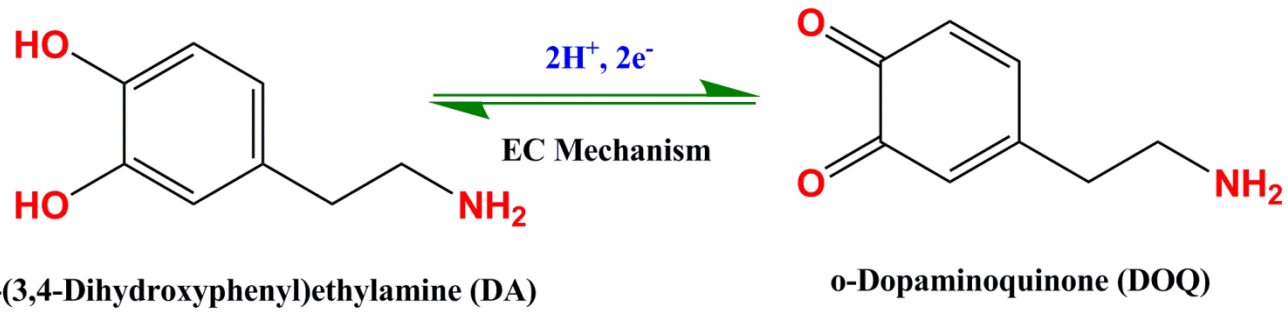

2-(3,4-Dihydroxyphenyl)ethylamine (DA) **o-Dopaminoquinone (DOQ)**

Scheme 2. Possible electrochemical redox mechanism of DA on the BaM modified SPCE.

3.3 Influence of scan rate and pH

To evaluate the electrochemical behavior of DA at ginger like BaM/SPCE, the effect of scan rate on the electrochemical oxidation of DA was examined by CV at various scan rates ranging from 10 to 200 mV/s (Fig.2B). As observed in Fig2B, the electrochemical oxidation (E_{pa}) and reduction (E_{pc}) peak potentials are slightly shifted towards anodic and cathodic direction while increasing the scan rate from lower to higher, suggesting that the characteristics of a quasi-reversible electrochemical redox reaction. Furthermore, the anodic peak currents (I_{pa}) and cathodic peak currents (I_{pc}) has a good linearity with scan rate (Fig.2C), the corresponding linear regression equation can be expressed as I_{pa} (μA) = 0.049 (mV/s) + 2.87, with a correlation coefficient of R^2 = 0.993, suggested that the electrochemical oxidation of DA on the ginger-like BaM/SPCE is an typically-adsorption controlled electrode process [36,37].

The electrochemical behavior (i.e., peak shape and current) of DA must be affected by changing the pH solution from (3-11), due to the contribution of protons in the overall electrode reaction. So that, the pH of electrolyte is most important analytical parameter in electrochemical studies, which can be directly affected the electrochemical activity of the proposed sensor. Thus, we have studied the electrochemical activity of DA in various pH solution. Fig.2D shows CV curves of BaM/SPCE (presence of 200 μM DA) with well-defined oxidization peak currents and the peak potentials were also shifted to the cathodic side upon increasing the pH values from 3.0 to 11.0. The oxidation peak currents of DA was gradually increased with increasing the pH values from 3.0 to 7.0, and then, peak current was gradually decreased when the pH values increasing above 7.0 (Fig.2F). The maximum oxidation peak current of DA was achieved at pH 7, so, we have chosen pH 7.0 as the favorable supporting electrolyte for the further electrochemical studies. Moreover, Fig.2E reveals the linear relationship between the peak potential and pH and the linear regression equation of E_{pa} = -0.061 + 0.67, with a correlation coefficient of R^2 = 0.993. From the linear plot of Fig.2E, the calculated slope value (61 mV/pH) is almost close to the Nernstian value (59 mV/pH). Hence, this result proved that the electrocatalytic oxidation of DA at the BaM/SPCE involves an equal number of electron and proton transfer reaction.

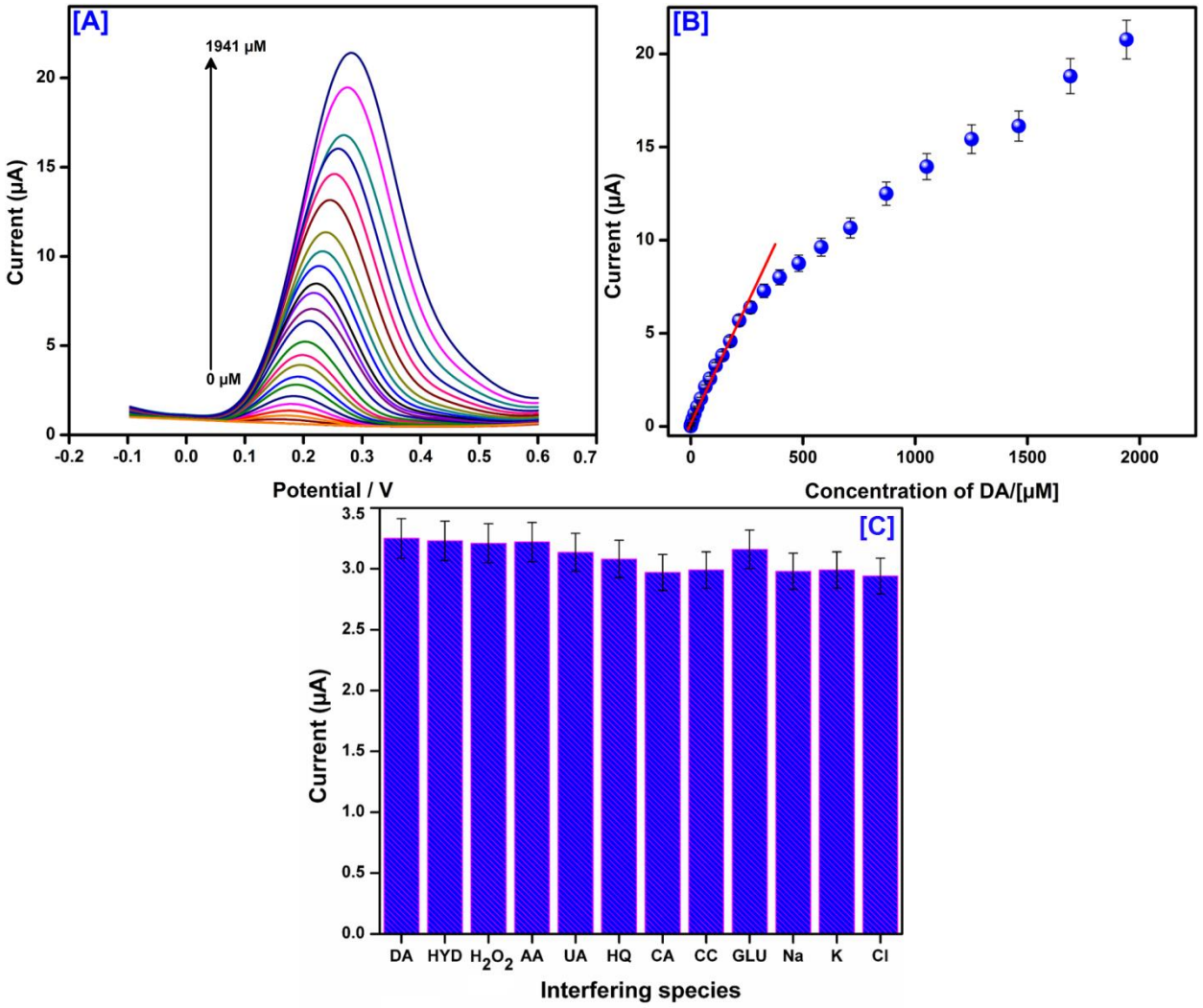

Figure 3. DPV of DA at BaM/SPCE in 0.05 M PBS (pH 7.0) with various concentrations from 0.1-1941 µM (A). The calibration plot for anodic peak current *vs.* concentration of DA (B). The interference studies at BaM/SPCE with presence of potentially co-interfering compounds: DA, HYD, H_2O_2, AA, UA, HQ, CA, CC, GLU, Na^+, K^+, and Cl^-.

3.4 Determination of DA on BaM/SPCE

DPV techniques is more sensitive tool to quantify the concentrations of DA, hence, the DPV was used to determine the DA. Fig.3A reveals the investigation of DA oxidation at the BaM modified SPCE in 0.05 M PBS (pH 7.0) with various concentrations of DA (0.1-1941 µM). A well-defined oxidation peak current was appeared while adding the concentrations from lower to higher at a potential of 0.18 V. However, the anodic peak current response was increased upon increasing the concentration of DA at BaM/SPCE in 0.05 M PBS (pH 7.0). Fig.3B shows the calibration plot for anodic peak current and concentrations of DA. The linear concentration range of the proposed sensor was obtained from 0.1 to 266 µM. The corresponding linear regression equation can be expressed as follows:

$$I_{pa}\,(\mu A) = 0.024\,(\mu M) + 0.26;\ (R^2 = 0.990) \quad (1)$$

Moreover, the modified electrode is proposed to have a lower detection limit of 0.021 µM and the electrode sensitivity was calculated to be 0.35 µA $\mu M^{-1}cm^{-2}$. In addition, the analytical performance such as LOD, linear response range and sensitivity of the BaM/SPCE modified electrode was potentially compared with previously reported other DA sensors and the results are given in Table 1[38-52]. From the results in Table 1, the proposed BaM/SPCE has an excellent analytical performance compared with other modified DA sensors. Therefore, the prepared BaM/SPCE possesses a very lower LOD, wide linear response range and good current sensitivity for the determination of DA.

Table 1. Comparison of analytical data for DA determination

Electrode	**Linear range (µM)**	**LOD (µM)**	**Ref.**
GNS-CNTs/MoS_2	0.1–100	0.05	[38]
pGr	0.005–200	0.001	[39]
Fe_2O_3 NPs/GRS	0.01–195	0.004	[40]
SPANI/CNSs/GCE	0.5–1780	0.015	[41]
GCE/N-rGO	0.5–170	0.250	[42]
GCE/Fe_2O/N-rGO_3	0.5–340	0.490	[43]
GR-CS/GCE	0.03-20	0.0045	[44]
MWCNT/[Cu(sal-ala)(bpy)]	0.1–300	0.16	[45]
pGO-GNP-pGO	0.1-30	1.28	[46]
Au/RGO/GCE	6.8-41	1.4	[47]
TiO_2-GR/GCE	5-200	2	[48]
Chitosan-GR/GCE	1-24	1	[49]
GR-AuNP/GCE	5-1000	1.86	[50]
GR/GCE	4-100	2.64	[51]
GO/GCE	1-15	0.27	[52]
Ginger-like BaM/SPCE	0.1-266	0.021	This work

3.5 Selectivity, stability, and repeatability studies

The selectivity of DA sensor is normally affected by the presence of co-interfering electroactive species such as AA, UA, GLU, HYD, H_2O_2, HQ, CA, CC, Na^+, K^+ and Cl^-. Hence, we have investigated that the sensing performance of DA in the presence of co-interfering compounds by DPV. The DPV response of DA was examined in the presence of 10-fold higher concentrations of co-interfering compounds (figure not shown). The oxidation peak current did not affect the peak current and peak potential of DA even in presence of 10-folds higher concentration of co-interfering compounds, suggests that the proposed BaM/SPCE has a well anti-interference capability. The bar diagram of Fig.3C, suggested that the prepared BaM modified SPCE has an excellent selectivity for the detection of DA.

The stability of the proposed BaM/SPCE modified electrode was examined in the presence of 100 μM DA containing 0.05 M PBS (pH 7.0) by DPV technique. The DA oxidation peak current response was slightly decreased (4.2 %) after 20^{th} cycles. After the 20^{th} cycles, there is no further oxidation peak current decrement was observed at BaM/SPCE, suggests that the proposed BaM/SPCE has an appreciable stability for the DA sensor. The repeatability was assessed through the consecutive measurements under DA for 5 times at a single BaM/SPCE with RSD of less than 5%, suggesting a good repeatability of the proposed sensor. These results revealed that the BaM/SPCE has a good stability, and repeatability for the DA sensor.

4. CONCLUSION

In this work we have successfully demonstrated a novel ginger-like $BaMoO_4$ by simple co-precipitation method. The as-prepared BaM modified SPCE was applied to the electrochemical detection of DA. The synthesized ginger-like BaM has a well-defined morphology and high crystallinity; it was thoroughly characterized by various analytical techniques such as XRD, FE-SEM, EDX, and Raman. The electrochemical detection of DA at the BaM modified SPCE was investigated by using CV and DPV techniques. Moreover, the fabricated electrode showed good linear response range (0.1-266 μM) and very lower detection limit (0.021 μM) for DA detection and the obtained results are effectively compared with previously reported articles. Moreover, the proposed BaM/SPCE exhibited an excellent selectivity, efficient electrocatalytic activity and good stability, for these peculiar properties and the excellent electrocatalytic activity behavior; it can be effectively used for further industrial applications.

ACKNOWLEDGMENTS
We would also like to acknowledge The Ministry of Science and Technology, Taiwan (MOST106-2221-E-182-021

References

1. L.Q. Mai, F. Yang, Y.L. Zhao, X. Xu, L. Xu, and Y.Z. Luo, *Nat. Commun*., 2 (2011) 381.
2. Y. Ding, S.H. Yu, C. Liu, and Z.A. Zang, *Chem. Eur. J.,* 13 (2007) 746-753.
3. Y.M. Zhang, F.D. Yang, J. Yang, Y. Tang, and P. Yuan, *Solid State Commun*., 133 (2005) 759-763.
4. A. Sen, and P. Pramanik, *Mater. Lett.,* 50 (2001) 287-294.
5. R. Karthik, J. Vinoth Kumar, S. M. Chen, C. Karuppiah, Y. H. Cheng, and V. Muthuraj, *ACS appl. mater. Interfaces*, *9*(7) (2017) 6547-6559.
6. R. Karthik, J. Vinoth Kumar, S.M. Chen, K. Seerangan, C. Karuppiah, T.W. Chen, and V. Muthuraj, *ACS appl. mater. Interfaces*, *9*(31) (2017) 26582-26592.
7. R. Karthik, J. Vinoth Kumar, S.M. Chen, T. Kokulnathan, H.Y. Yang, and V. Muthuraj, *ACS Sustain. Chem. Eng*., 6(7) (2018) 8615-8630.
8. V.B. Mikhailik, and H. Kraus, *Phys. Status Solidi B,* 247 (2010) 1583-1599.
9. J.A. Groenink, C. Hakfoort, and G. Blasse, *Phys. Status Solidi A*, 54 (1979) 329-336.
10. Y. Yin, Y. Gao, Y. Sun, B. Zhou, L. Ma, X. Wu, and X. Zhang, *Mater. Lett.,* 64 (2010) 602-604.
11. J.H. Ryu, J.W. Yoon, C.S. Lim, W.C. Oh, and K. Bo Shim, *J. Alloys Compd*., 390 (2005) 245-249.
12. C. Pupp, R. Yamdagni, and R.F. Porter, *J Inorg Nucl Chem.*, 31 (1969) 2021-2029.
13. Y. Sun, J. Ma, J. Fang, C.Gao, and Z. Liu, *Ceramics International*, 37 (2011) 683-686.

14. C.T. Xia, V.M. Fuenzalida, and R.A. Zarate, *J Alloy Compd.,* 316 (2001) 250-255.
15. Y. Mi, Z.Y. Huang, F.L. Hu, and X.Y. Li, *Mater Lett.,* 63 (2009) 742-744.
16. A.P. De Azevedo Marques, D.M.A. de Melo, C.A. Paskocimas, P.S. Pizani, M.R. Joya, E.R. Leite, and E. Longo, *J Solid State Chem.,* 179 (2006) 671-678.
17. C. Zhang, E.H. Shen, E.B. Wang, Z.H. Kang, L. Gao, C.W. Hu, and L. Xu, *Mater Chem Phys.*, 36 (2006) 240-243.
18. P. Afanasiev, *Mater Lett.*, 61 (2007) 4622-4626.
19. J.H. Ryu, J.W. Yoon, C.S. Lim, and K.B. Shim, *Mater Res Bull.*, 40 (2005) 1468-1476.
20. A. Pandikumar, G. Soon How, T. See, F. Omar, S. Jayabal, K. Kamali, and N. Yusoff, *RSC Adv.*, 4 (2014) 63296-63323.
21. G. Di Chiara, V. Bassareo, S. Fenu, M. De Luca, L. Spina, C. Cadoni, E. Acquas, E. Carboni, V. Valentini, and D. Lecca, *Neuropharmacology*, 47 (2004) 227-241.
22. M. Mazloum-Ardakani, H. Rajabi, H. Beitollahi, B. B. F. Mirjalili, A. Akbari, and N. Taghavinia, *Int. J. Electrochem. Sci.*, *5* (2010) 147-157.
23. Z. Zhuang, J. Li, R. Xu, and D. Xiao, *Int. J. Electrochem. Sci.*, *6* (2011) 2149-2161.
24. N. Hassanzadeh, and H. R. Zare-Mehrjardi, *Int. J. Electrochem. Sci.*, *12* (2017) 3950-3964.
25. S. Zheng, R. Huang, X. Ma, J.Tang, Z. Li, X. Wang, and J. Wang, *Int. J. Electrochem. Sci.*, *13* (2018) 5723-5735.
26. V. Mani, R. Devasenathipathy, S.M. Chen, K. Kohilarani, and R. Ramachandran, *Int. J. Electrochem. Sci.*, *10* (2015).1199-1207.
27. N. Karikalan, M. Velmurugan, S.M. Chen, and K. Chelladurai, *RSC Adv.*, *6*(54) (2016) 48523-48529.
28. R. Nehru, and S.M. Chen, *RSC Advances*, *8*(49) (2018) 27775-27785.
29. J. Vinoth Kumar, R. Karthik, S.M. Chen, N. Karikalan, K. Chelladurai, C.C. Yang, and V. Muthuraj, A*CS Appl. Mater. Interfaces*, 10 (2018) 15652-15664.
30. R. Karthik, N. Karikalan, S.M. Chen, J. Vinoth Kumar, C. Karuppiah, and V. Muthuraj, *J. Catal.,* 352 (2017) 606-616.
31. G.H. Bouchard Jr, and M.J. Sienko, *Inorg. Chem.*, *7*(3) (1968) 441-443.
32. A. Phuruangrat, T. Thongtem, and S. Thongtem, *J. Phys. Chem. Solids*, *70*(6) (2009) 955-959.
33. J.V. Kumar, R. Karthik, S.M. Chen, T. Kokulnathan, S. Sakthinathan, V. Muthuraj, and T.W. Chen, *Inorg. Chem*., *5*(3) (2018) 643-655.
34. C. Zhang, L. Zhang, C. Song, G. Jia, S. Huo, and S. Shen, *J. Alloy. Comp., 589* (2014) 185-191.
35. P.A.G. O'Hare, *J. Chem. Thermodyn.*, *6*(5) (1974) 425-434.
36. R. Karthik, K. Saravanakumar, S.M. Chen, J.V. Kumar, C.M. Lee, B.S. Lou, V. Muthuraj, A. Elangovan, and S. Kulandaivel, *Int. J. Electrochem. Sci.,* 12 (2017) 1474-1491.
37. M. Velmurugan, N. Karikalan, S.M. Chen, Y.H. Cheng, and C. Karuppiah, *J. Colloid Interface sci.*, *500* (2017) 54-62.
38. V. Mani, M. Govindasamy, S.M. Chen, R. Karthik, and S.T. Huang, *Microchim. Acta*, 183 (2016) 2267-2275.
39. A. Ramachandran, S. Panda, and S.K. Yesodha, *Sens. Actuator B-Chem.*. 256 (2018) 488-497.
40. T. Kokulnathan, S.M. Chen, V. Chinnuswamy, and K. Kadirvelu, *Inorg Chem Front.*, 5 (2018) 705-718.
41. Y. Fu, Q. Sheng, and J. Zheng, *New J Chem.*, 41 (2017) 15439-15446.
42. P. Wiench, Z. González, R. Menéndez, B. Grzyb, and G. Gryglewicz, *Sens. Actuator B-Chem.*, 257 (2018) 143-153.
43. Z. Yang, X. Zheng, and J. Zheng, *J. Alloys Compd.*, 709 (2017) 581-587.
44. S. Palanisamy, K. Thangavelu, S.M. Chen, P. Gnanaprakasam, V. Velusamy, and X.H. Liu, *Carbohydr Polym.*, 151 (2016) 401-407.
45. S. Sakthinathan, S.M. Chen, and W.C. Liao, *Inorg Chem Front,*, 4 (2017) 809-819.
46. S.S. Choo, E.S Kang, I. Song, D. Lee, J.W. Choi, and T.H. Kim, *Sensors*, 17 (2017) 861.

47. C. Wang, J. Du, H. Wang, C.E. Zou, F. Jiang, P. Yang, and Y. Du, *Sens. Actuators B Chem.*, 204 (2014) 302-309.
48. Y. Fan, H.T. Lu, J.H. Liu, C.P. Yang, Q.S. Jing, Y.X. Zhang, X.K. Yang, and K.J. Huang, *Colloids Surf. B Biointerfaces*, 83 (2011) 78-82.
49. D. Han, T. Han, C. Shan, and A. Ivaska, *Electroanalysis*, 22 (2010) 2001-2008.
50. J. Li, J. Yang, Z. Yang, Y. Li, S. Yu, Q. Xu, and X. Hu, *Anal. Methods*, 4 (2012) 1725-1728.
51. Y.R. Kim, S. Bong, Y.J. Kang, Y. Yang, R.K. Mahajan, J.S. Kim, and H. Kim, *Biosens. Bioelectron.*, 25 (2010) 2366-2369.
52. F. Gao, X. Cai, X. Wang, C. Gao, S. Liu, F. Gao, and Q. Wang, Q. *Sens. Actuators B Chem.*, 186 (2013) 380-387.